Spin dynamics in $Sr_{14}Cu_{24}O_{41}$ from ^{63}Cu NQR-NMR and susceptibility measurements

P. Carretta, S. Aldrovandi, and R. Sala
Department of Physics ''A. Volta,'' Unitá INFM and Sezione INFN di Pavia-Via Bassi, 6-27100-I Pavia, Italy

P. Ghigna
INCM-Department of Physical Chemistry, Via Taramelli 16, - 27100-I Pavia, Italy

A. Lascialfari
Department of Chemistry, Via Maragliano 75/77- 50144-I Firenze, Italy
(Received 18 July 1996; revised manuscript received 17 June 1997)

^{63}Cu NMR-NQR relaxation measurements in oriented powders of $Sr_{14}Cu_{24}O_{41}$, in the temperature range 4.2 K$\leqslant T\leqslant$600 K and for magnetic-field intensities up to 9.4 T, are presented. This compound has a complex structure comprising alternating layers containing $Cu(1)O_2$ chains and $Cu(2)_2O_3$ two-leg ladders. At high temperatures $^{63}Cu(2)$ nuclear relaxation rates probe the $Cu(2)^{2+}$ spin dynamics in the two-leg ladders and an overall agreement with the theoretical predictions for the temperature and field dependence of T_1 and T_{2G} is observed. In particular, $1/T_1 \propto \ln(1/\omega_e \pm \omega_R)$, with ω_e the electron Larmor frequency and ω_R the nuclear resonance frequency. At low temperatures ($T\leqslant$150 K), an extra contribution to $^{63}Cu(2)$ NMR-NQR relaxation rates is observed and tentatively related to the $Cu(1)^{2+}$ correlated spin dynamics. In this temperature range the magnetic field is observed to cause an anomalous reduction of $1/T_1$, $1/T_{2G}$, and of the dc susceptibility. The analysis of the temperature dependence of the $^{63}Cu(2)$ NQR frequency evidences a stabilization in the local lattice distortions below $\simeq$85 K, where also $Cu(1)^{2+}$ spin dimerization is observed. The relevance of these distortions in driving the $Cu(1)^{2+}$ spin dimerization is thus discussed. [S0163-1829(97)06646-0]

I. INTRODUCTION

After the discovery of high-T_c superconductivity a renewed interest in low-dimensional quantum magnetism[1] has emerged also in view of a possible role of the spin excitations in the pairing mechanism. Furthermore, due to recent progress in the chemical synthesis of the cuprates it is now possible to obtain the best model Heisenberg $S=1/2$ chain (Sr_2CuO_3),[2,3] two-($SrCu_2O_3$) and three-leg-ladder ($Sr_2Cu_3O_5$) (Ref. 4) systems and one can now study the changeover of the spin dynamics in quantum Heisenberg magnets on passing almost continuously from one to two dimensions. Also the recent discovery of a spin-Peierls (SP) state in $CuGeO_3$,[5] and its complex magnetic-field-temperature phase diagram has stimulated the study of one-dimensional antiferromagnetism and has also sparked interest in the problematics related to lattice assisted spin dimerization and dimerization processes associated with competing nearest-neighbor (NN) and next-nearest-neighbor (NNN) superexchange interactions.[6]

$Sr_{14}Cu_{24}O_{41}$ is an insulator having an incommensurate structure formed by alternating layers with $Cu(1)O_2$ chains, Sr ions and $Cu(2)_2O_3$ two-leg ladders[7] (see Fig. 1). Therefore it appears as an interesting system where one can investigate at the same time the spin dynamics in the chains, where $Cu(1)^{2+}$ spins are weakly coupled via $\simeq$94° superexchange bondings (J'), and in the two-leg ladders where the strong superexchange coupling (J) causes the opening of a gap of hundreds of degrees Kelvin between singlet and triplet states. As regards the spin excitations in the ladders some controversy is present due to unexpected differences in the values of the gap estimated from dc susceptibility and NMR T_1 measurements.[4] However, these estimates are based on analytical approximations which should be valid only for temperatures $T\ll\Delta$,[8] Δ being the amplitude of the gap between singlet and triplet excitations. In order to clarify this point a comparison between quantum Monte Carlo[9] calculations, which should correctly estimate also the high-temperature behavior of NMR-NQR T_1 and T_{2G}, and the experimental data over a wide temperature range appears more appropriate. Furthermore, due to the peculiar features in the density of states of the low-energy excitations, a logarithmic divergence of $1/T_1$ should be observed on decreasing the field intensity. For these reasons we have performed $^{63}Cu(2)$ NMR-NQR T_1 and T_{2G} measurements over a wide

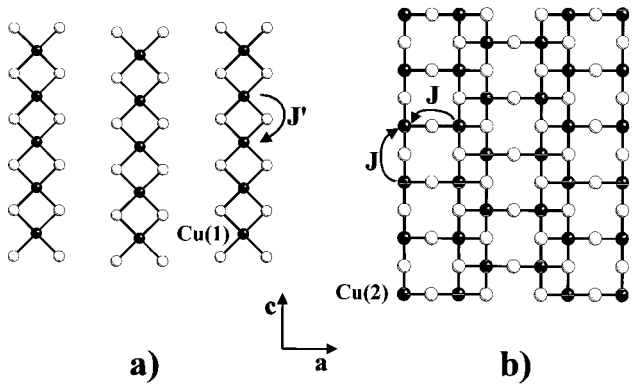

FIG. 1. The two layers of the $Sr_{14}Cu_{24}O_{41}$ structure, comprising $Cu(1)O_2$ chains (a) and $Cu(2)_2O_3$ two-leg ladders (b). J' is the superexchange coupling along the chains, while J is the one in the two-leg ladders. Open circles represent oxygen ions, while the black circles represent copper ions. The b axis is perpendicular to the plane of the page.

temperature range ($4.2 \leqslant T \leqslant 600$ K) and for different magnetic-field intensities. We observed an overall agreement with the theoretical numerical predictions for the temperature dependence of nuclear spin-lattice relaxation rate (NSLRR) and nuclear spin-spin relaxation rate of ^{63}Cu(2) for $150 \leqslant T \leqslant 600$ K [at lower temperatures ^{63}Cu(2) T_1 and T_{2G} are related to $Cu(1)^{2+}$ spin dynamics]. We have also observed the expected logarithmic divergence of $1/T_1$ on decreasing the field intensity, $1/T_1 \propto \ln(1/\omega_e \pm \omega_R)$ with ω_e the electron Larmor frequency and ω_R the nuclear resonance frequency.

Also the spin excitations in the $Cu(1)O_2$ chains are characterized by the opening of a gap around 85 K originating from $Cu(1)^{2+}$ spin dimerization, as pointed out recently by Matsuda and Katsumata.[10] According to these authors the dimerization is not assisted by lattice distortions, as for $CuGeO_3$, but is due to competing NN and NNN superexchange interactions. However, the peculiar temperature dependence of ^{63}Cu(2) nuclear quadrupole resonance frequency and the peak in $1/T_1$ observed at $T \simeq 85$ K could suggest that lattice distortions could be relevant for the dimerization mechanism. Finally, we observed an anomalous reduction of the dc susceptibility and of the NMR-NQR relaxation rates at low temperatures.

The manuscript is divided as follows: in Sec. II we describe the sample preparation, characterization, and the experimental details of dc susceptibility and NQR-NMR measurements. In Sec. III we present and discuss the experimental results. In Sec. IV the summarizing remarks and conclusions are given.

II. EXPERIMENTAL

A. Sample preparation and characterization

$Sr_{14}Cu_{24}O_{41}$ was prepared by solid-state synthesis starting from CuO (Fluka puriss. p. a.) and $SrCO_3$ (Aldrich $>98\%$). The starting materials were weighted in the required stoichiometric ratio, suspended in acetone and mixed overnight. The acetone was evaporated and the resulting powder was pressed isostatically at 2000 bars to yield a compact pellet. The pellet was then heated in a platinum crucible at 800 °C in a pure oxygen flux for 76 h with two intermediate grinding and pressing steps. The completion of the chemical reaction and the homogeneity of the as prepared material was checked by XRPD and microscopic (optical scanning electron microscopy and electron microprobe analysis) inspection. The oxygen content of the as prepared materials was measured to be 41.0 by following the weight loss occurring in the reaction at 500 °C with a flowing mixture of hydrogen in argon (7% H_2) with a TA Thermal Analyst 2000 apparatus equipped with a thermogravimetric analyzer attachment. A platinum pan was employed as a sample holder.

X-ray diffraction patterns (XRPD) were taken on a Philips 1710 diffractometer, operating at 40 KV and 35 mA, equipped with a Cu radiation tube, adjustable divergence slit, graphite monocromator on the diffracted beam and proportional detector. A homemade environmental chamber[11] was employed in the high-temperature experiments. The lattice constants were determined by minimizing the weighted differences between calculated and experimental Q_i, with $Q_i = (2 \sin\theta_i/\lambda_i^2)^2$, and weight $\sin^{-2}(2\theta_i)$.[12] Instrumental aberrations were considered by inserting additional terms in the linear least-squares model. The indexing scheme was taken from Ref. 13.

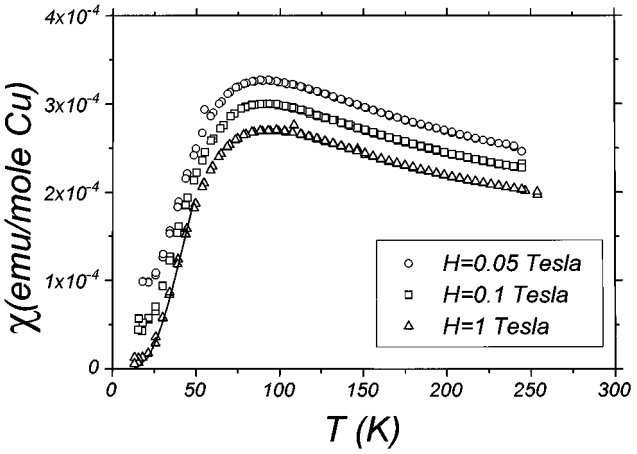

FIG. 2. Temperature dependence of the dc spin susceptibility after subtracting a Curie term $\chi_C = C/T$ with $C = 0.0127$ emu K/mole Cu, for different field intensities. The solid line shows the activated behavior for a gap $\Delta' = 120$ K.

dc susceptibility measurements were performed by using a Metronique Ingegnerie superconducting quantum interference device M03 magnetometer, equipped with an 8 T superconducting magnet and operating in the range $2-300$ K. The technique of measurement is based on the displacement of a sample inside a second-order gradient meter, which gives a signal with a peak-to-peak amplitude proportional to the sample magnetization. Hereafter we will call susceptibility the quantity $\chi = M/H$ which, in principle , can differ from $(dM/dH)_H$. In fact, M is observed to slightly saturate on increasing the field intensity (see Fig. 2). The total spin susceptibility is the sum of a Curie C/T term associated with defects and of the susceptibility due to $Cu(1)O_2$ chains and $Cu(2)_2O_3$ ladders. Since the gap for the spin excitations in the two-leg ladders is rather high ($\Delta \simeq 600$ K, see later on), for $T \leqslant 300$ K only $Cu(1)^{2+}$ spins contribute significantly to the spin susceptibility. From the low-temperature fit of the total susceptibility we estimate $C = 0.0127$ K emu/mole Cu, corresponding to $\simeq 3\%$ of Cu^{2+} impurity spins, presumably originating from the chain open ends. The Van Vleck and diamagnetic contributions to the total susceptibility were estimated to be negligible.[14,10]

B. NMR and NQR experimental aspects

^{63}Cu NMR and NQR measurements have been carried out either with Bruker MSL 200, Bruker AMX400 or with homemade pulse spectrometers. NMR measurements have been performed in oriented powders with grains aligned with the b axis parallel to the external magnetic field, while NQR measurements have been performed in unoriented powder samples sealed in pyrex ampoules in order to avoid modifications in the oxygen stoichiometry during the high-temperature ($T \geqslant 400$ K) measurements. NQR ($\pm 3/2 \rightarrow \pm 1/2$) and NMR spectra were obtained by monitoring the echo amplitude on changing the irradiation frequency, with rf power kept at moderate levels in order to minimize the artificial broadening of the lines. In NMR the length of the $\pi/2$

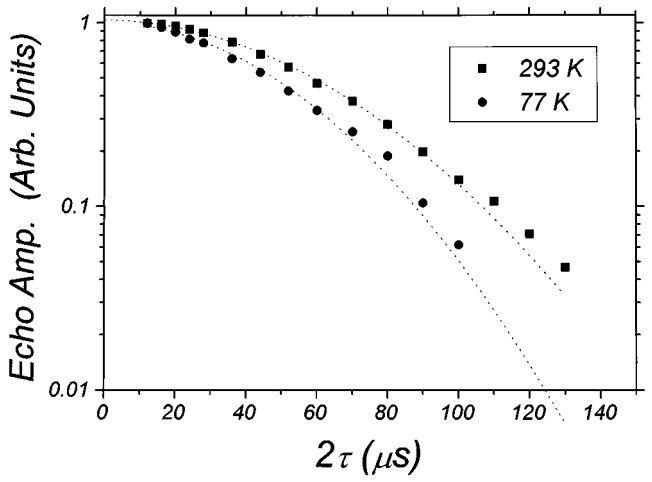

FIG. 3. Decay of the echo amplitude for the central ^{63}Cu(2) NMR line as a function of the delay τ between the rf pulses, for $T=293$ and 77 K and $H=5.9$ T parallel to the b axis. The dotted lines are the best fits according to Eq. (1) in the text.

pulses when irradiating the central ^{63}Cu(2) $1/2\rightarrow -1/2$ line was observed to be slightly shorter than the one for the $\pm 3/2\rightarrow\pm 1/2$ satellite lines and nearly half of that of ^{63}Cu in thin metallic copper wires, as expected. In order to reduce the magnetoacoustic ringing we used during T_2 measurements or when recording the NMR and NQR spectra the following phase cycling: $(xy+,-xy-,-xx+,xx-)$, where $\pm x$ and $\pm y$ are the phases of the rf pulses, while the sign $\pm$ at the end gives the phase of the receiver. Using this pulse sequence and by using appropriate silver coils we could reduce the dead time of the acquisition to 8 μs in NQR and down to 4 μs in NMR.

The decrease in the echo amplitude on increasing the delay τ between the two pulses was observed to be Gaussian over nearly two decades (Fig. 3), due to a strong contribution from the indirect spin-spin coupling and to a small contribution from T_1 processes, especially at low temperatures. Following Pennington *et al.*[15] we have divided the decay of the echo amplitude into an exponential term related to Redfield contribution and a Gaussian one associated with nuclear direct and indirect dipolar coupling, namely,

$$E(2\tau)=E(0)\exp\left(-\frac{2\tau}{T_{2R}}\right)\exp\left[-\frac{1}{2}\left(\frac{2\tau}{T_{2G}}\right)^2\right] \qquad (1)$$

with $1/T_{2R}=(1/T_1)_\perp+(a/T_1)_\parallel$, where $\parallel$ and $\perp$ are with respect to the quantization axis of the nucleus [b axis for Cu(2) NMR-NQR measurements], while $a=2$ for NQR and 3 for NMR when irradiating the central line. The anisotropy ratio of T_1 at room temperature was evaluated $(T_1)_\parallel/(T_1)_\perp=3.9\pm 0.2$. Although for a very anisotropic $1/T_1$ the estimate of $(1/T_1)_\perp$ can suffer from uncertainties due to some misalignment in the sample orientation, we would like to stress that these corrections have a minor influence, being $1/T_{2G}\gg 1/T_{2R}$. In order to avoid oscillations in the decay of the echo amplitude due to residual external fields, we protected the sample chamber with a μ-metal tube during the T_{2G} measurements in NQR. The length of the pulses in the NMR measurements allowed a complete irradiation of the whole ^{63}Cu(2) central line (linewidth at half intensity $\Delta\nu\simeq 70$ kHz), while in NQR all or slightly less than the whole line ($\Delta\nu\geqslant 280$ kHz) was irradiated during the T_{2G}, measurements. This fact is not believed to affect the estimate of T_{2G}, since on reducing the amplitude of the rf field down to 50% no effect on the value of T_{2G} was detected. Furthermore, we mention that in NQR the decay rate after a $\pi/2-\tau-\pi/2$ pulse sequence was the same as that after a $\pi/2-\tau-\pi$ sequence, evidencing possible contributions from dynamical processes involving fluctuations of unlike nuclear spins.[16]

Nuclear-spin-lattice-relaxation rate $1/T_1=2W$ was estimated from the recovery of the nuclear magnetization after saturation with a comb of rf pulses, or after inversion of the population on the $\pm 1/2$ levels for ^{63}Cu(2) NMR $1/T_1$ at the central line. In order to avoid magnetoacoustic ringing or long-time instabilities in the electronics we used a pulse sequence with immediate subtraction of $m(\infty)$,[17] the signal obtained after a complete recovery of the nuclear magnetization. For ^{63}Cu(2) the recovery of nuclear magnetization was observed to follow the recovery laws derived in the case of a magnetic relaxation mechanism, namely

$$y(t)=\frac{m(\infty)-m(t)}{m(\infty)}=\exp(-6Wt) \qquad (2)$$

in NQR [see Fig. 4(a)]

$$y(t)=0.1\exp(-2Wt)+0.9\exp(-12Wt) \qquad (3)$$

for the central NMR line [see Fig. 4(b)], and

$$y(t)=0.1\exp(-2Wt)+0.5\exp(-12Wt)+0.4\exp(-6Wt) \qquad (4)$$

for the NMR satellites [see Fig. 4(c)]. We checked at 77 and 293 K, by comparing ^{63}Cu and ^{65}Cu $1/T_1$, that the relaxation mechanism was indeed of magnetic nature. Since the asymmetry parameter of the electric field gradient for ^{63}Cu(2) nuclei $\eta\simeq 0.6$ (see Sec. III A), the eigenstates in NQR are no longer the $|m_z=\pm 3/2\rangle$ and $|m_z=\pm 1/2\rangle$ but they are a linear combination of all $|m_z\rangle$ states. Thus one could suspect that Eq. (2) is not adequate to describe the recovery of nuclear magnetization in this case, even though, one can observe that unless $\eta\simeq 1$ the factor in the exponential of Eq. (2) is rather close to $6W$. In the case of ^{63}Cu(1) the recovery of the nuclear magnetization after saturating the NMR line at 66.65 MHz was observed to follow a stretched exponential, possibly due to electric-field-gradient inhomogeneities which prevent the occurrence of a common spin temperature among ^{63}Cu(1) nuclei. On the other hand, since the estimate of ^{63}Cu(1) $1/T_1$ is affected by the presence of the underlaying tails of ^{63}Cu(2) NMR spectrum (see Fig. 5), due to some distribution in the orientation of the grains, meaningful values for ^{63}Cu(1) relaxation rates can hardly be obtained. Therefore, in the following, we will comment only on the experimental results for ^{63}Cu(2) NMR-NQR relaxation rates. Experiments on single crystals would be required to investigate ^{63}Cu(1) NMR relaxation rates.

III. EXPERIMENTAL RESULTS AND DISCUSSION

A. NMR-NQR spectra and electric-field gradients (EFG)

The ^{63}Cu room-temperature NMR spectrum is shown in Fig. 5. One observes a broad line around Larmor frequency

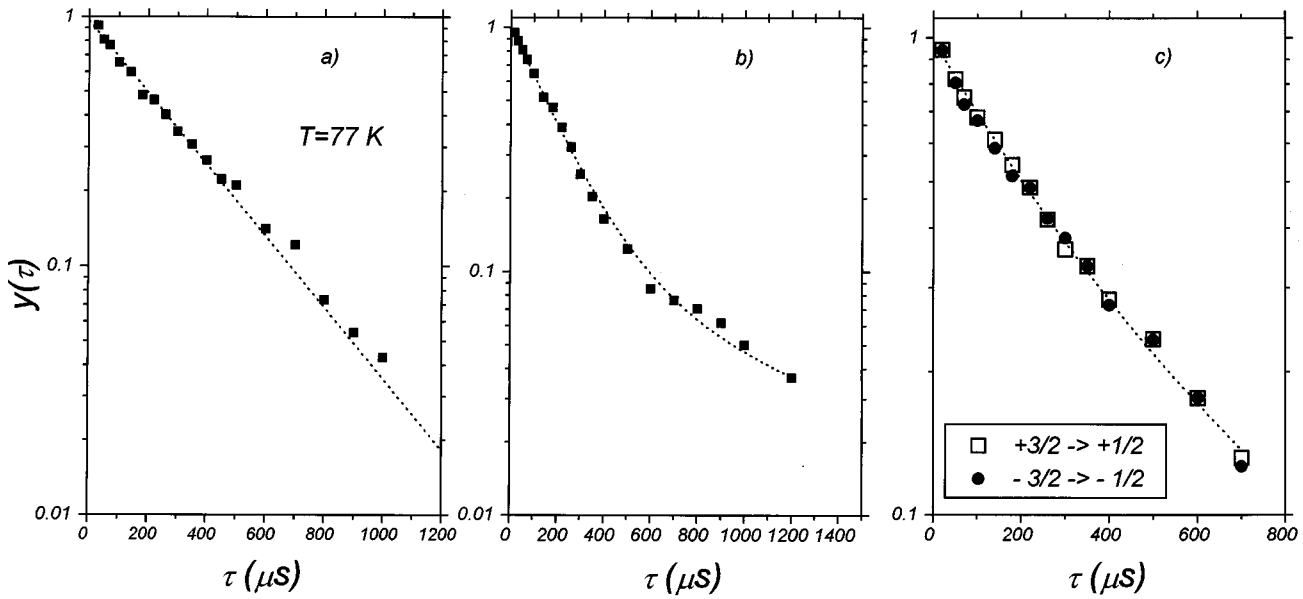

FIG. 4. Recovery plots for the nuclear magnetization after saturating the ^{63}Cu(2) NQR line at $T=77$ K (a) and the NMR satellite lines at $T=293$ K (c), or after inverting the population of the $\pm 1/2$ levels, for ^{63}Cu(2) NMR central line at $T=293$ K (b). The dotted lines in (a), (b), and (c) show the best fits according to Eqs. (2), (3), and (4) in the text, respectively.

and a shifted narrow central line, with two satellites separated by ± 14.3 MHz. From the shift of the satellites and by comparison with the NQR frequency [15.3 MHz at room temperature (see Fig. 6)] one deduces that one of the two species of ^{63}Cu nuclei has a quadrupolar frequency $\nu_Q = 14.3 \pm 0.1$ and an asymmetry parameter of the EFG ($Z \| b$) $\eta = 0.66 \pm 0.03$. On the basis of point-charge calculations we can attribute these EFG parameters to ^{63}Cu(2). Although an approach based on a point-charge model is questionable in metallic compounds it has proven to explain quite well the EFG values in insulating cuprates.[18] In this approximation one can write the total EFG tensor as

$$V_{\mathrm{tot}} = (1-\gamma_\infty) V_{\mathrm{ion}} + V_{3d}\,, \tag{5}$$

where the first term describes the contribution from the lattice ions, $(1-\gamma_\infty)$ being the Sternheimer antishielding factor, while the second term is the one from valence or ligand electrons. In the calculation of the second term we will neglect contributions from electrons on orbitals other than the $3d$ ones, thus[19,18]

$$(V_{3d})^{\alpha\beta} = (1-R) e \int \psi_{3d}^{*} \frac{3\alpha\beta - \delta_{\alpha\beta} r^2}{r^5} \psi_{3d} d\tau (\alpha, \beta = x, y, z) \tag{6}$$

with $(1-R) \simeq 1$ the Sternheimer shielding factor. By using standard values for the Sternheimer antishielding factor [$(1-\gamma_\infty) = 20.8$] and considering that the contribution to the EFG from a hole in a $3d_{x^2-y^2}$ orbital is $\simeq 76$ MHz,[18] we could reproduce the values of ν_Q and η ($Z \| b$) on the basis of point-charge calculations for a ground state of the $3d^9$ hole $\psi_{3d} = 0.998 |3d_{x^2-y^2}\rangle + 0.03 |3d_{z^2}\rangle$. One can qualitatively associate the small admixture of $3d_{z^2}$ wave function to the small orthorombic distortion in Cu(2) coordination. Similar calculations carried out for Cu(1) site give a value of $\nu_Q \simeq 3$ MHz and a value of η close to unity for a purely $3d_{x^2-y^2}$ ground state, causing an uncertainty in the definition of the Z axis of the EFG. A more precise analysis, however, would require the knowledge of the correct symmetry of the ground-state wave function. We point out that also for the ''zig-zag chain compound'' $SrCuO_2$,[20] where the local coor-

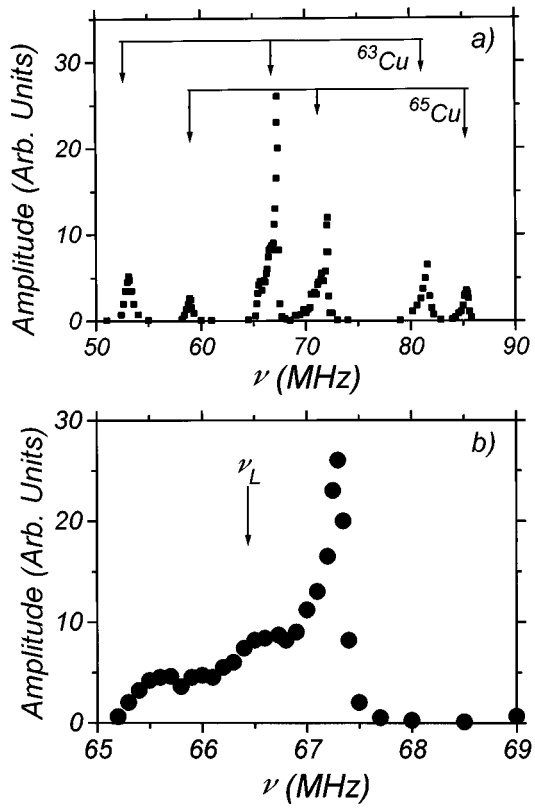

FIG. 5. (a) ^{63,65}Cu NMR spectrum for $H=5.9$ T parallel to the b axis. The arrows in the center indicate ^{63,65}Cu(2) central line and the broad ^{63,65}Cu(1) NMR spectrum. The arrows on the two sides show ^{63,65}Cu(2) NMR satellite lines. (b) The central ^{63}Cu(2) NMR line and the broad ^{63}Cu(1) NMR spectrum are shown in an expanded scale. The arrow indicates Larmor frequency.

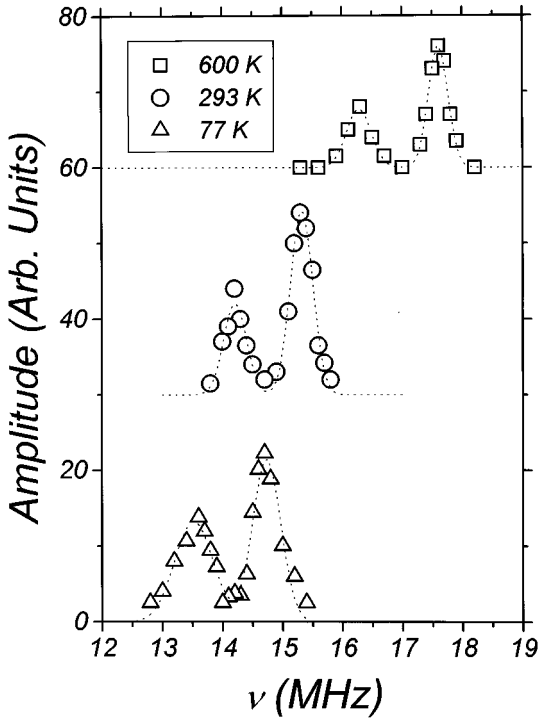

FIG. 6. ^{63,65}Cu(2) NQR spectra at three different temperatures. A little broadening of the lines is observed on decreasing temperature. The Gaussian dashed lines are guides to the eye.

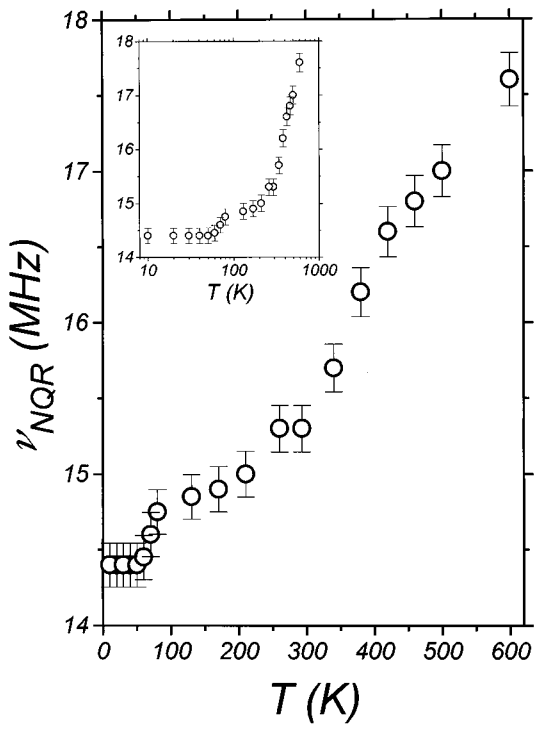

FIG. 7. Temperature dependence of the resonance frequency for ^{63}Cu(2) NQR line in $Sr_{14}Cu_{24}O_{41}$. In the inset the same plot is shown with the x axis in logarithmic scale in order to evidence the stabilization of the NQR resonance frequency below 80 K.

dination of Cu is similar to that of Cu(1), ^{63}Cu ν_Q is small. In further support of this assignment of NQR-NMR spectra we mention that the temperature dependence of ^{63}Cu $1/T_1$ (see later on) when irradiating the NQR line around 15 MHz or the narrow NMR central line, which was attributed to Cu(2), is very similar to the one for ^{63}Cu in the two-leg-ladder compound $SrCu_2O_3$.[21]

The temperature dependence of ^{63}Cu(2) NQR frequency is reported in Fig. 7. One observes a strong temperature dependence of ν_{NQR} above room temperature, while on decreasing temperature one observes a stabilization around 85 K. The strong temperature dependence could be associated, in principle, to the thermal expansion of the lattice parameters (see Fig. 8). However, on the basis of point charge calculations, considering the temperature dependence of the lattice parameters reported in Fig. 8 and assuming no change in the direct coordinates of the ions in the lattice, we derive an increase of ν_{NQR} by less than 1% on changing the temperature from 293 to 520 K, much less than the modification experimentally detected. Thus we deduce that the observed temperature dependence of ^{63}Cu(2) ν_{NQR} originates from distortions in the local structure around Cu(2) ions. These lattice distortions may cause, in principle, two important effects: modify the hyperfine coupling constants and/or modify the superexchange coupling and the spin-excitation spectrum.

The lattice distortions can also affect the temperature dependence of the ^{63}Cu(2) magnetic hyperfine shift ΔK (Fig. 9), either by modifying the hyperfine coupling constants or the orbital term which is related to the splitting of the crystal-field levels. In order to derive information on the orbital contribution to the hyperfine shift one has first to subtract the spin contribution which provides information on the hyperfine coupling constants. We assume an electron-nucleus Hamiltonian of the Mila-Rice[22] form for ^{63}Cu(2), neglecting the coupling to $Cu(1)^{2+}$, as it seems appropriate for $T \gtrsim 110$ K. Then one can write

$$\mathcal{H} = \gamma\hbar \vec{I} A \vec{S} + \gamma\hbar \vec{I} \sum_{i=1}^{3} B \vec{S}_i , \tag{7}$$

where the first term is the on-site hyperfine coupling while the second one is the transferred hyperfine coupling from the three nearest-neighbor (NN) Cu^{2+} spins in the same ladder.

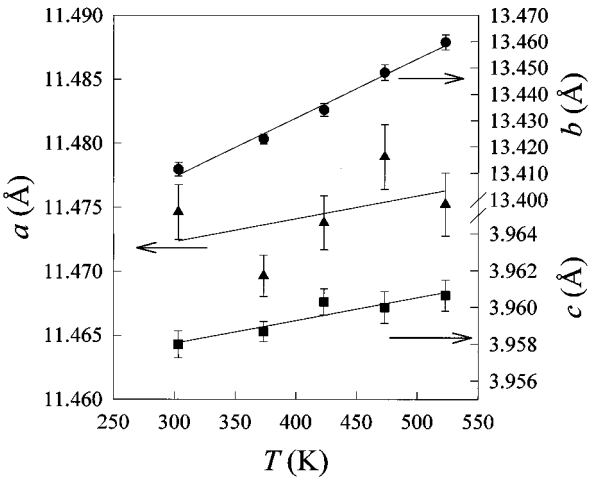

FIG. 8. Temperature dependence of the lattice parameters above room temperature, obtained from the XRD patterns.

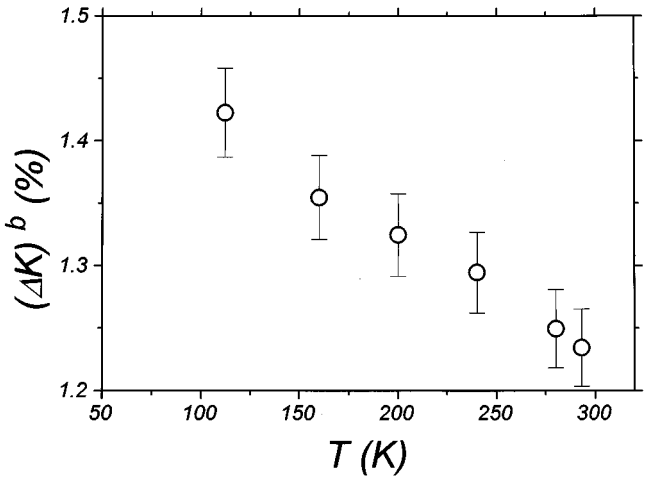

FIG. 9. Temperature dependence of ^{63}Cu(2) NMR shift for $H=5.9$ T parallel to the b axis.

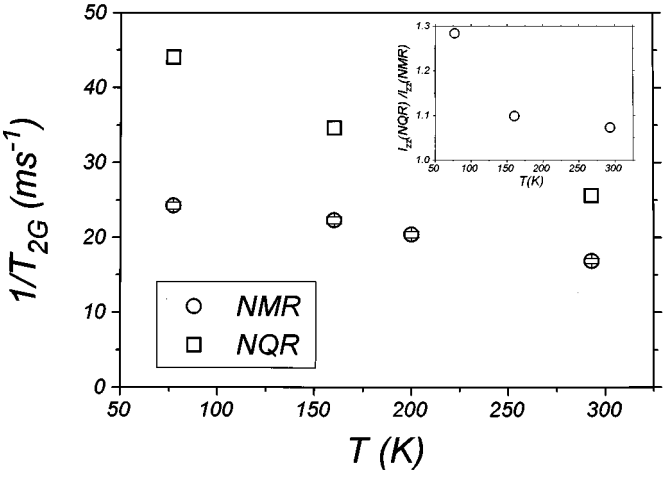

FIG. 10. Temperature dependence of ^{63}Cu(2) Gaussian decay rate $1/T_{2G}$ in NQR and in NMR (central line), for $H=5.9$ T along the b axis. In the inset the ratio between the q-integrated spin susceptibilities $I_{zz}=\Sigma_{\vec{q}}C_{\vec{q}}^4[\chi'_{zz}(\vec{q},0)]^2-[\Sigma_{\vec{q}}C_{\vec{q}}^2\chi'_{zz}(\vec{q},0)]^2$ for NQR and NMR is reported.

The assumption that the transferred hyperfine term is due just to three NN rather than four is not relevant since $B\simeq 0$, as it will be shown in the following (for further discussion see Sec. III C). Then one can write the hyperfine shift tensor in the form

$$\Delta K=(A+3B)\frac{M}{H}+\Delta K_{\rm orb}, \tag{8}$$

with M the local magnetization due to the $Cu(2)^{2+}$ spins in the two-leg ladders [the macroscopic one at low temperatures is dominated by $Cu(1)^{2+}$ spin susceptibility] and $\Delta K_{\rm orb}$ is the orbital contribution to the shift. The temperature dependence of ΔK is mainly due to the temperature dependence of M and is expected to be similar to that observed for ^{63}Cu in $SrCu_2O_3$. However, two important differences with respect to $SrCu_2O_3$ are observed (see Fig. 9 and Refs. 4 and 21): (a) the low-temperature value of ΔK is certainly higher, implying a higher value for the orbital part of the shift; (b) the variation of ΔK from room temperature to 110 K is larger than for $SrCu_2O_3$. Point (a) indicates a modification in the low-temperature crystal-field splitting for Cu(2) with respect to $SrCu_2O_3$, in particular being

$$(\Delta K_{\rm orb})^b=\frac{16\mu_B^2\langle r^{-3}\rangle}{E_{xy}-E_{x^2-y^2}} \tag{9}$$

for a hole in $3d_{x^2-y^2}$ ground state, assuming $(\Delta K_{\rm orb})^b=1.45\%$ one can estimate a crystal-field splitting between d_{xy} and $d_{x^2-y^2}$ states of 2.35 eV. Point (b) can be explained on the basis of a stronger global $(A+3B)$ hyperfine coupling for $\vec{H}\|b$, causing a more sizeable temperature dependence of ΔK. If we assume for $Sr_{14}Cu_{24}O_{41}$ the same temperature dependence of the local magnetization in the ladders as for $SrCu_2O_3$ we derive a global coupling constant $(A+3B)_b=-310\pm 20$ kOe, which, by assuming an on-site term similar to the one in other cuprates,[18,23] indicates a value of B close to zero. One could suspect that the stronger temperature dependence observed in $Sr_{14}Cu_{24}O_{41}$ is related to changes in the hyperfine constant and/or orbital term originating from structural deformations, however, based on the temperature dependence of the NQR frequency we can assert that these modifications are rather small in the temperature range $100\leqslant T\leqslant 300$ K.

B. Transverse relaxation rate $1/T_{2G}$

The ^{63}Cu(2) transverse relaxation rate $1/T_{2G}$, derived from the decay of the echo amplitude [see Eq. (1)], is much higher than the one associated with the direct nuclear dipole interaction and is related to the indirect nuclear dipole coupling via the localized Cu^{2+} magnetic moments. In this case one can express the transverse relaxation rate in terms of the real part of the static spin susceptibility $\chi'_{zz}(q,0)$ along the quantization axis[15] ($z\equiv b$)

$$\left(\frac{1}{T_{2G}}\right)^2=\frac{0.69}{\delta}\hbar^2\gamma^4\left\{\frac{1}{N}\sum_{\vec{q}}C_{\vec{q}}^4[\chi'_{zz}(\vec{q},0)]^2-\left[\frac{1}{N}\sum_{\vec{q}}C_{\vec{q}}^2\chi'_{zz}(\vec{q},0)\right]^2\right\} \tag{10}$$

with $\delta=4$ for NQR and $\delta=8$ for NMR when irradiating the central line, and $C_{\vec{q}}=[A_b+B+2B\cos(q_xa)]$. In Fig. 10 one observes that on decreasing temperature $1/T_{2G}$ increases either for NQR or for NMR. The rate of this increase should be related not only to that of the increasing correlations but also to the ratio between B and $A_\parallel$. In particular, by comparing the temperature depndence of ^{63}Cu(2) NMR $1/T_{2G}$ with the quantum Monte Carlo calculations by Sandvik *et al.*[9] we observe a good agreement for $B/A_b\simeq 0$, supporting our previous observations based on shift measurements. It is interesting to notice that the ratio between $1/T_{2G}$ in NQR and in NMR is higher than the factor $\sqrt{2}$ expected from the difference in the constant δ [see Eq. (10)] for the two cases and keeps increasing on decreasing temperature (see Fig. 10). The increase of $1/T_{2G}$ on decreasing the field intensity is analogous to the one detected in dc susceptibility measurements and therefore one is tempted to attribute it to an indirect contribution to $1/T_{2G}$ from $Cu(1)^{2+}$ spins. Namely, the

total ^{63}Cu(2) nuclear spin-spin relaxation rate due to indirect processes should be written as

$$(1/T_{2G})^2=(1/T_{2G})^2_{\mathrm{Cu}(2)}+(1/T_{2G})^2_{\mathrm{Cu}(1)}, \tag{11}$$

where the first term is the one described in Eq. (10) with $\chi_{zz}(q,0)$ the spin susceptibility associated with $Cu(2)^{2+}$ spins, while the second one involves $Cu(1)^{2+}$ spin susceptibility and is depressed by the magnetic field. It is clear that in this case ^{63}Cu(2) nuclear dipoles interact via $Cu(1)^{2+}$ spins through a non-negligible transfered hyperfine coupling as happens for the Cu nuclei in the chains $YBa_2Cu_3O_{7-x}$, for instance.[23] On the other hand, in principle, other spin-spin relaxation processes involving Cu(1) nuclear or electronic spins are possible. For example, the process could be a dynamical one associated with the slowing down of $Cu(1)^{2+}$ spin fluctuations to frequencies of the order of the inverse of the echo delay τ; or it could be related to Cu(1)-Cu(2) nuclear dipolar coupling giving a contribution to ^{63}Cu(2) spin-spin relaxation once the T_1 of ^{63}Cu(1) is close to τ. However, the second process cannot explain the order of magnitude of the enhancement of $1/T_{2G}$ while the first one would require $Cu(1)^{2+}$ spin fluctuation frequencies of the order of 10 kHz, which is quite unlikely. Furthermore, one would expect a modification in the function describing the decay of the echo amplitude, a fact which is not experimentally observed. Therefore, the only process which appears plausible with our observations originates from the indirect coupling between ^{63}Cu(2) nuclear spins via $Cu(1)^{2+}$ spins.

The field-induced decrease of $(1/T_{2G})_{\mathrm{Cu}(1)}$ could originate either from a reduction in the q-integrated spin susceptibility $\chi_{zz}(q,0)$ (see the inset in Fig. 10), possibly associated with a quenching in the amplitude of spin fluctuations along the magnetic field, or to a reduction in the hyperfine coupling constants. The contribution of $Cu(1)^{2+}$ spins to ^{63}Cu(2) $1/T_{2G}$ is temperature dependent and is strongly enhanced around 85 K. This enhancement, also observed in $1/T_1$ (see Fig. 11), is possibly related to an enhancement in the amplitude of field fluctuations in proximity of the dimerization temperature and could involve also modifications in the hyperfine coupling constants due to the lattice distortions.

C. Nuclear spin-lattice relaxation rate (NSLRR) $1/T_1$

The temperature dependence of ^{63}Cu(2) NQR and NMR (at 5.9 T and for $\vec{H}\|b$) NSLRR is shown in Fig. 11. One notices that, for $T\gtrsim 150$ K, $1/T_1$ follows an activated behavior, however, a clear difference in the values obtained from NMR and NQR measurements is observed. At low temperatures one can observe a clear peak in the NQR NSLRR which is strongly depressed in NMR. In order to clarify these effects one has to understand the relevance of the magnetic field intensity in measuring $1/T_1$. We will first discuss the high-temperature ($T\gtrsim 150$ K) behavior of NSLRR which is dominated by $Cu(2)^{2+}$ spin dynamics.

NSLRR can be expressed in terms of the components of the dynamical structure factor, $S_{i=x,y,z}(\vec{q},\omega)=\int_{-\infty}^{\infty}\langle S^i_{\vec{q}}(t)S^i_{\vec{q}}(0)\rangle e^{i\omega t}dt$ $(z\|H_0\|b)$, in the form

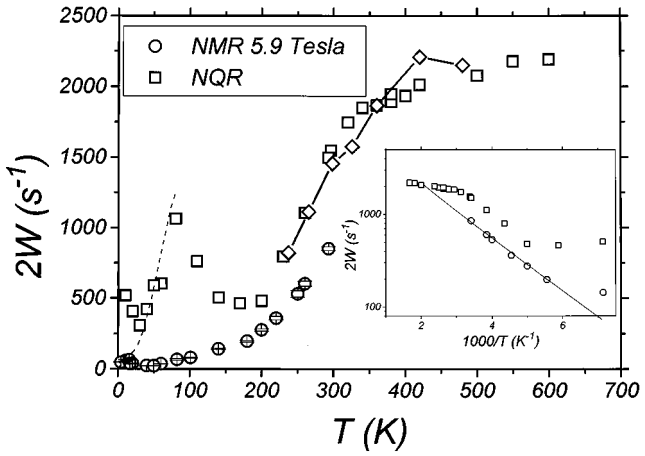

FIG. 11. Temperature dependence of the ^{63}Cu(2) NSLRR $2W$ in NQR and in NMR for $H=5.9$ T parallel to the b axis. In the inset the same data are shown in an Arrhenius plot, the solid line giving the behavior expected for a gap $\Delta(\pi/a)=650$ K. The dashed line at low temperatures shows the activated behavior for a dimerization gap $\Delta'=120$ K, the same derived from dc susceptibility data (see in the text and in Fig. 2). The diamonds connected by the solid line show the results from quantum Monte Carlo calculations taken from Fig. 2 in Ref. 9, for $J=1200$ K and $B/A_{\mathrm{ac}}=0$, after rescaling by the appropriate hyperfine coupling constant.

$$1/T_1=\frac{\gamma^2}{2N}\sum_{\vec{q}}\left[A_z(\vec{q})^2S_z(\vec{q},\omega_R)+A_\perp(\vec{q})^2S_\perp(\vec{q},\omega_e\pm\omega_R)\right], \tag{12}$$

where $A_{\perp,z}(\vec{q})$ are form factors describing the hyperfine coupling of the spin excitations at wave vector $\vec{q}$ to the nuclei. The hyperfine coupling tensor for ^{63}Cu(2) nuclei is diagonal in the frame of reference of the crystallographic axes and is dominated by the on-site contribution. Then, only the second term of the above equation is present, with $A_\perp(\vec{q})=[A_{\mathrm{ac}}+B+2B\cos(q_xa)]$. In two-leg ladders, dimerized chains or Haldane gap systems, at low temperatures and low magnetic fields ($g\mu_BH/k_B\ll T\ll\Delta$), only the low part of the triplet magnon branch is populated. In that case, following Sagi and Affleck,[24] the nuclear relaxation is dominated by indirect $q\simeq 0$ processes which can be either intrabranch ($\Delta m_z=0$) ones, described by the first term of Eq. (12) [absent for ^{63}Cu(2)], or interbranch ($\Delta m_z=\pm 1$) ones where a simultaneous flip of the electron and nuclear spins occur [second term of Eq. (12)]. Then the temperature dependence of $1/T_1$ for $T\ll\Delta$ is an activated one, the value of $1/T_1$ increasing with the increasing population of triplet states.[8,24] By assuming a quadratic dispersion relation for magnons at $k_x\simeq\pi/a$ Troyer *et al.*[8] found for $T\ll\Delta$

$$1/T_1\simeq\frac{d\gamma^2}{2NJ}\times\exp\left(-\frac{\Delta}{k_BT}\right)\times(A^2_\perp)_{q=0}[0.8909+\ln(k_BT/\hbar(\omega_e\pm\omega_R)]. \tag{13}$$

The above expression fits quite well the temperature dependence of $1/T_1$ from 150 to $\simeq 320$ K for a value of the gap $\Delta(\pi/a)\simeq 650$ K (see the inset to Fig. 11). The deviations observed at higher temperatures should be attributed to the fact that the quadratic approximation for the magnon disper-

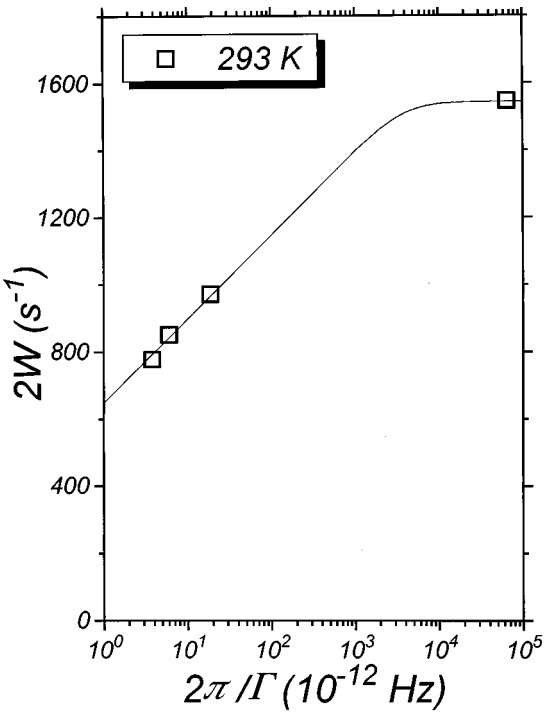

FIG. 12. $2W$ for ^{63}Cu(2) as a function of $2\pi/\Gamma$, with $\Gamma=\omega_e \pm \omega_R$ for $T=293$ K. The line shows the function $1/T_1 = \alpha \ln(k_B T/\hbar\Gamma\sqrt{1+(\omega_c/\Gamma)^2})$ [see Eq. (13)], with $\omega_c/2\pi = 2.7 \times 10^8$ Hz, a low-frequency cutoff.

sion relation is no longer valid as $T\rightarrow\Delta$, since also excitations at $k_x<\pi/a$, where the dispersion curve is more linear, become relevant. For this dispersion form, following the same calculations reported in Ref. 8 one would derive $1/T_1 \propto T\exp(-\Delta/T)$. Even though, a more complete analysis of the high temperature behavior has to take into account all possible processes including those in the continuum of the spin excitations. This analysis has been carried out by Sandvik *et al.* using the quantum Monte Carlo technique.[9] We observe that using the hyperfine constants adequate for this compound, the trend of NSLRR can be fairly well reproduced assuming $J\simeq 1200$ K for the superexchange along and between the two chains of a ladder and considering $B/A_{ac} \simeq 0$ for the ratio between the hyperfine coupling constants (see Fig. 11). In this case, when both superexchange couplings along and between the chains forming the ladder are equal, one should expect $\Delta(\pi/a)=J/2\simeq 600$ K,[25] which is in reasonable agreement with our estimate from the analysis of T_1 for $150\leqslant T\leqslant 320$ K using the expression in Eq. (13).

At this point, having clarified the temperature dependence of Cu(2) NSLRR for $T\geqslant 150$ K we have to understand the effect of the magnetic field in depressing its amplitude. As it appears from Eq. (13) $1/T_1$ should increase logarithmically on decreasing the field intensity, i.e., on decreasing $\Gamma=\omega_e \pm \omega_R \simeq \omega_e$. In fact we observe that on varying the field intensity between 9.4 and 1.9 T, $1/T_1$ progressively increases (Fig. 12). The field dependence is well described by Eq. (13) and the slope of the function plotted in Fig. 12 does not have any adjustable parameter. A small frequency cutoff, possibly related to interladder couplings and/or to a spin anisotropy, was introduced. In NQR Γ is much smaller than in NMR and a pronounced increase of ^{63}Cu(2) $1/T_1$ is observed when the field intensity is decreased from 1.9 T to zero.

In order to check if $1/T_1$ in NMR diverges as $\ln(k_B T/\hbar\Gamma)$ instead of $\ln(k_B T/\hbar\omega_R)$ we did the following analysis. While in the first case $1/T_1$ measured either on the central line or on the satellites should be the same with the recovery laws given by Eqs. (3) and (4), respectively, in the second case the transition probabilities between the Zeeman states are frequency dependent and the recovery laws should be modified accordingly. At room temperature and for a magnetic field of 5.9 T, where most of the experiments were performed, the coefficients $2W, 6W$, and $12W$ in Eqs. (3) and (4) should be replaced by $2.036W^h$, $6.119W^h$, and $12.213W^h$, with $2W^h$ the relaxation rate for the high-frequency satellite. We found that when the experimental data were fitted according to Eqs. (3) and (4) W was the same for all lines within ± 2 % [see Fig. 4(c)], while when the corrected expression was used a slightly larger disagreement was found and W^h was observed to vary within ± 4%. Despite the fact that the above analysis does not appear to give a definite answer, we point out that when the field is reduced from 1.9 T to zero $1/T_1 \equiv 2W$ varies by a factor $\simeq 2$, as expected for $1/T_1 \propto \ln(k_B T/\hbar\Gamma)$, while if it varied according to $\ln(k_B T/\hbar\omega_R)$ an increase by only 4% should be observed. A more precise definition of the curve in Fig. 12 could have been obtained from Zeeman-perturbed NQR measurements. However, in order to obtain significant data long statistics (around 10^6-10^7 averages) and a good stability of the whole experimental apparatus (cryostat and spectrometer) over more than one week are required to obtain one point. Since such a stability was hardly achievable we did not perform these measurements.

At high temperatures ^{63}Cu(2) NQR $1/T_1$ reaches asymptotically a value close to 2200 s^{-1}, not too different from the asymptotic value 2600 s^{-1} for ^{63}Cu $1/T_1$ in La_2CuO_4.[26] In the high-temperature limit $T\gtrsim J$ one has

$$1/T_1 = \frac{\gamma^2}{4}(A_{ac}^2 + nB^2)\frac{\sqrt{2\pi}}{\omega_{exc}}, \qquad (14)$$

with n the effective number of NN electron spins which are coupled to ^{63}Cu(2) nuclei via the transferred hyperfine term B and $\omega_{exc}=[2J^2k_B^2mS(S+1)/3\hbar^2]^{1/2}$ Heisenberg exchange frequency, m being the number of NN electron spins coupled via the superexchange coupling J. It is clear that in general $m\neq n$ and the assumption that $n=m$ should be valid only if the electrons involved in the strong superexchange coupling, namely, those in Cu $3d$ and O $2p$ orbitals, are also the ones causing the transferred hyperfine coupling. Now, this is not true in general and in particular one should understand which is the role played by $4s$ electrons in the transferred hyperfine coupling.[18] For this reason we find also reasonable the assumption $n=4$, while $m=3$. Even though, this assumption does not affect the analysis of the temperature dependence of NSLRR since adjacent spin ladders are equivalent and causes minor differences in the estimate of the absolute values of $1/T_1$ since B is rather small. Thus, by taking into account in estimating ω_{exch} that $J=1200$ K and $m=3$ one derives, for $1/T_1(T\gg J)=2200$ s^{-1} and $B\simeq 0$, an hyperfine coupling constant $A_{ac}\simeq 120$ kOe, in reasonable agreement with the estimates for ^{63}Cu in other spin-ladder compounds.[21] We also point out that for this coupling constant

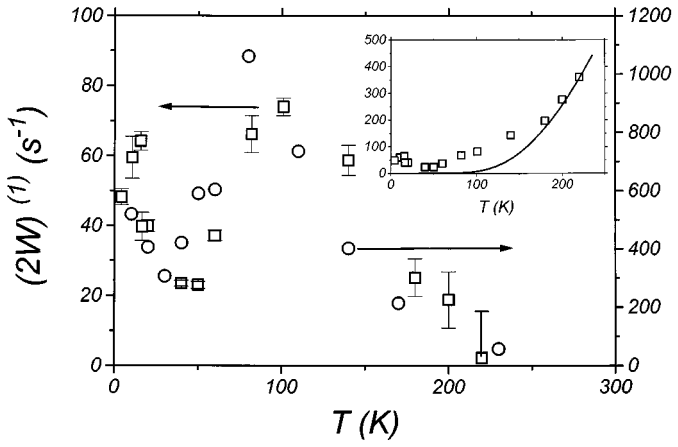

FIG. 13. NSLRR for ^{63}Cu(2) after subtracting the activated contribution from $Cu(2)^{2+}$ spin fluctuations [see Eq. (13)] with a gap $\Delta = 660$ K, for $H = 0$ (NQR) and $H = 5.9$ T parallel to the b axis. The vertical scale for NQR data (circles) is the one on the right, while the vertical scale for NMR data (squares) is the one on the left. In the inset the raw data for ^{63}Cu(2) NSLRR are shown (see Fig. 11) together with the activated high-temperature behavior (solid line) obtained for a gap $\Delta = 660$ K.

one would get an anisotropy of $1/T_1$ of $\simeq 3.83$, very close to the one experimentally observed (see Sec. II B).

After having discussed the high-temperature behavior of ^{63}Cu(2) $1/T_1$ we turn now to the discussion of the behavior for $T \leqslant 150$ K, which is possibly related to the $Cu(1)^{2+}$ spin dynamics. ^{63}Cu(2) NQR $1/T_1$ shows a well-defined peak of magnetic origin around 85 K. This peak could be associated with a slowing down of the field fluctuations associated with the softening of the vibrational modes in correspondence of a lattice distortion and is not the critical one associated with a transition to a magnetically ordered phase since no average hyperfine field at the nuclei is detected below 85 K. The peak is remarkably depressed by the application of a magnetic field, but it is not absent. In fact, if we subtract from ^{63}Cu(2) $1/T_1$ the high temperature activated trend [see Eq. (13)] associated with the $Cu(2)^{2+}$ spin dynamics one observes (Fig. 13) that NMR and NQR NSLRR have the same temperature dependence but are different in magnitude by a factor $\simeq 15$. At first one could suspect that this peak is associated to the slowing down in the diffusive motion of the extra holes intrinsically present due to the three excess oxygens of $Sr_{14}Cu_{24}O_{41}$, the hopping rate becoming of the order of the Larmor frequency around 85 K. However, the observed field dependence of $1/T1$ is much stronger than the one expected for relaxation processes associated with diffusive holes.[27] Furthermore, taking into account that the gap between localized and itinerant states estimated from transport measurements is around $E_g = 0.18$ eV,[14] the characteristic hopping time of the holes,[27] $\tau_h = \tau_o \times \exp(Eg/T)$ with $\hbar \tau_0^{-1}$ of the order of the bandwidth, should become of the order of nuclear Larmor frequency at much higher temperatures. If one had τ_h^{-1} of the order of ω_L at 85 K one would get a $\tau_0 < 10^{-18}$ s, which is too small.

The marked reduction of $1/T_1$ could also indicate that the magnetic field causes a remarkable suppression in the amplitude of field fluctuations at ^{63}Cu(2) nuclei $\perp$ to $\vec{H}$ possibly due to a quenching in the amplitude of $Cu(1)^{2+}$ spin fluctuations parallel to the applied magnetic field or to a modification in the hyperfine coupling constants through a magnetocrystalline coupling. Even if a dipolar hyperfine coupling could support the first observation it will be in contrast with the previous findings from T_{2G} measurements, namely the external magnetic field cannot quench both the amplitude of field fluctuations along and perpendicular to the magnetic-field direction. Furthermore, these two effects should cause a decrease in $1/T_1$ of the order of those observed in $1/T_{2G}$ and dc susceptibility measurements, which, however, is an order of magnitude smaller. Hence, the remarkable effect of the magnetic field on $1/T_1$ should have a different origin. One could suspect that the field dependence of NSLRR is the classical one associated to long time diffusive tails in the $Cu(1)^{2+}$ spin-correlation function,[28] giving for a one-dimensional system $1/T_1 \propto 1/\sqrt{H}$ for $T \gtrsim J'$. The value of J' along the CuO_2 chains should be of the order of a hundred of Kelvin degrees and it is possible that the system is no longer in the classical limit for $T \simeq 80$ K. However, as recently pointed out by Takigawa *et al.*[29] it is possible that this diffusive behavior extends to temperatures below J'. The relevant field dependence of $1/T_1$ should be attributed to relatively small values of the diffusion constant $D \simeq \omega_{\rm exc}$ and of the interchain coupling causing the low-frequency cutoff.

At low temperatures a small peak in $1/T_1$ is still present. This peak is not a critical one, since no anomaly in the low-temperature specific-heat measurements is detected, but should be possibly attributed to a freezing in the spin fluctuations associated with the hopping around a CuO_2 plaquette of the already localized extra holes, similar to what is observed in other cuprates.[27]

IV. SUMMARIZING REMARKS AND CONCLUSIONS

From the comprehensive analysis of ^{63}Cu(2) NMR-NQR measurements we have achieved insights on the correlated $Cu(2)^{2+}$ (two-leg-ladder site) and $Cu(1)^{2+}$ (chain site) spin dynamics, the first dominating the ^{63}Cu(2) relaxation processes at high temperatures ($T \gtrsim 150$ K), while the latter the low-temperature ones. As regards the contribution from $Cu(2)^{2+}$ spins we have observed the following:

(a) The temperature dependence of $1/T_1$ is in good agreement with theoretical calculations up to temperatures $T \simeq \Delta$, assuming an intraladder superexchange coupling $J \simeq 1200$ K, along and between the two chains forming the ladder.

(b) $1/T_1 \propto \ln(1/\omega_e \pm \omega_R)$, and we demonstrated that $1/T_1$ probes $S(\vec{q}, \omega_e \pm \omega_R)$.

(c) From the temperature dependence of the NMR shift, $1/T_{2G}$ and $1/T_1$ we estimated the following coupling constants between ^{63}Cu(2) nuclei and $Cu(2)^{2+}$ spins: $A_b \simeq -310$ kOe, $A_{\rm ac} \simeq 120$ kOe, and $B \simeq 0$.

Unfortunately for this compound there is not the possibility of comparing the gap estimated from dc susceptibility with the one derived from $1/T_1$ measurements, the first being dominated by the response from $Cu(1)^{2+}$ spins.

On the other hand, for what concerns $Cu(1)^{2+}$ spin dynamics we mention the following:

(a) The temperature dependence of the dc susceptibility, combined with the absence of a magnetic order, indicates a

dimerization of $Cu(1)^{2+}$ spins below $\simeq 85$ K.[10,14] The absolute values of the dc susceptibility, $1/T_{2G}$ and $1/T_1$, are depressed by the magnetic field.

(b) The onset of the dimerization coincides with a stabilization in the $^{63}Cu(2)$ NQR frequency, pointing out that around 85 K there is a stabilization of the local lattice structure.

(c) At nearly the same temperature ($\simeq 85$ K) we observe a peak in $1/T_1$.

These observations could suggest that the spin dimerization is influenced by lattice distortions. In fact, if a dimerization takes place the superexchange coupling along the chains J' has to be negative and this is unlikely for 90° superexchange bondings which usually give a small ferromagnetic coupling. Therefore, one should expect that the lattice distortions cause an increase in the Cu-O-Cu bonding angle on decreasing the temperature towards $\simeq 85$ K. In particular, for a chain of weakly interacting dimers one would expect $J' \simeq \Delta' \simeq 120$ K. This coupling constant is close to the one of $CuGeO_3$,[30] implying that the superexchange angles possibly increase to values $\Theta \simeq 100-120°$. On the other hand, a more accurate determination of the lattice parameters by neutron-scattering measurements would be required. Finally, to elucidate the origin of the anomalous reduction of the dc susceptibility and $^{63}Cu(2)$ NMR-NQR relaxation rates induced by the magnetic field $^{63}Cu(1)$ NMR measurements in single crystals are necessary. Although further measurements are required to gain a more clear scenario, we have clearly evidenced the presence of anomalous properties in $Cu(1)^{2+}$ spin excitations in CuO_2 chains and pointed out that relevant lattice distortions occur before the chain spins dimerize.

ACKNOWLEDGMENTS

Useful discussions with A. Rigamonti, F. Borsa, D. Gatteschi, and A. Caneschi are gratefully acknowledged. A.L. would like to thank A. Caneschi for his technical assistance during dc susceptibility measurements. This research has been carried out with the financial support of INFN (Istituto Nazionale di Fisica Nucleare) and of INFM (Istituto Nazionale di Fisica della Materia).

[1] E. Dagotto and T. M. Rice, Science **271**, 619 (1995).
[2] T. Ami *et al.*, Phys. Rev. B **51**, 5994 (1995); S. Eggert, *ibid.* **53**, 5116 (1996).
[3] M. Takigawa *et al.*, Phys. Rev. Lett. **76**, 4612 (1996).
[4] M. Azuma *et al.*, Phys. Rev. Lett. **73**, 3463 (1994).
[5] M. Hase, I. Terasaki, and K. Uchinokura, Phys. Rev. Lett. **70**, 3651 (1993).
[6] See, for example, K. Okamoto, H. Nishimori, and Y. Taguchi, J. Phys. Soc. Jpn. **55**, 1458 (1986): N. Katoh and M. Imada, *ibid.* **63**, 4529 (1994), and references therein.
[7] E. M. McCarron *et al.*, Mater. Res. Bull. **23**, 1355 (1988).
[8] M. Troyer, H. Tsunetsugu, and D. Würtz, Phys. Rev. B **50**, 13 515 (1994).
[9] A. Sandvik, E. Dagotto, and D. J. Scalapino, Phys. Rev. B **53**, R2934 (1996).
[10] M. Matsuda and K. Katsumata, Phys. Rev. B **53**, 12 201 (1996).
[11] U. Anselmi Tamburini, G. Campari, P. Ghigna, and G. Spinolo, Powder Diffr. **8**, 210 (1993).
[12] U. Anselmi Tamburini and G. Spinolo, J. Appl. Crystallogr. **26**, 5 (1993).
[13] D. W. Wong-Ng *et al.*, Joint Commitee for Powder Diffraction Standards (JCPDS) Report No. 39-489 (1988).
[14] M. Kato *et al.*, Physica C **235-240**, 1327 (1994); M. W. McElfresh *et al.*, Phys. Rev. B **40**, 825 (1989).
[15] C. H. Pennington, D. J. Durand, C. P. Slichter, J. P. Rice, E. Bukowski, and D. M. Ginsberg, Phys. Rev. B **39**, 274 (1989).
[16] R. E. Walstedt and S. W. Cheong, Phys. Rev. B **51**, 3153 (1995).
[17] C. Berthier *et al.*, Appl. Magn. Reson. **3**, 449 (1992).
[18] T. Shimizu *et al.*, Bull. Magn. Reson. **12**, 39 (1990).
[19] A. Abragam, in *Principles of Nuclear Magnetism* (Clarendon, Oxford, 1961).
[20] K. Ishida *et al.*, Phys. Rev. B **53**, 2827 (1995).
[21] K. Ishida *et al.*, J. Phys. Soc. Jpn. **63**, 3222 (1994).
[22] F. Mila and T. M. Rice, Physica C **157**, 561 (1989).
[23] S. E. Barrett *et al.*, Phys. Rev. B **41**, 6283 (1990).
[24] J. Sagi and I. Affleck, Phys. Rev. B **53**, 9188 (1996).
[25] T. Barnes *et al.*, Phys. Rev. B **47**, 3196 (1993).
[26] T. Imai *et al.*, Phys. Rev. Lett. **70**, 1002 (1993); P. Carretta, A. Rigamonti, and R. Sala, Phys. Rev. B **55**, 3734 (1997).
[27] P. Carretta, M. Corti, and A. Rigamonti, Phys. Rev. B **48**, 3433 (1993); **49**, 7044 (1994), and references therein.
[28] H. Benner and J. P. Boucher, in *Magnetic Properties of Layered Transition Metal Compounds*, edited by L. J. De Jongh (Kluwer, Dordrecht, 1990), p. 323.
[29] M. Takigawa *et al.*, Phys. Rev. Lett. **76**, 2173 (1996).
[30] G. A. Petrakovskii *et al.*, Sov. Phys. JETP **71**, 772 (1990).